Creating Thermal Icons - A Model Based Approach

ANSHUL SINGHAL, Massachusetts Institute of Technology
LYNETTE A. JONES, Massachusetts Institute of Technology

The objective of this set of experiments was to evaluate thermal pattern recognition on the hand and arm and to determine which features of thermal stimuli are encoded by cutaneous thermoreceptors and perceived by the user of a thermal display. Thermal icons were created by varying the direction, rate and magnitude of change in temperature. It was found that thermal icons were identified more accurately when presented on the thenar eminence or the wrist, as compared to the fingertips and that thermal patterns as brief as 8 s could be reliably identified. In these experiments, there was no difference in performance when identifying warm or cool stimuli. A dynamic model of the change in skin temperature as a function of the thermal input was developed based on linear system identification techniques. This model was able to predict the change in skin temperature from an unrelated experiment involving thermal icons. This opens the possibility of using a model-based approach to the development of thermal icons.

General Terms: Design, Experimentation, Human factors, Measurement, Performance, Theory

Additional Key Words and Phrases: thermal display, thermal feedback, thermal perception, hand–object interaction

ACM Reference format:

Singhal, A., and Jones, L. A., 2017. Thermal Pattern Identification. *ACM Trans. Appl. Percept*. X, X, Article XX (May 2017), 20 pages. DOI: XX.XXXX/XXXX

1 INTRODUCTION

There is increasing interest in using the cutaneous senses as a medium of communication in many types of mobile devices and consumer products to provide feedback regarding the success of an action or to inform the user about some aspect of the external environment. Tactile communication systems represent a promising arena for enhancing the display of information in situations in which the visual and auditory systems are overloaded. To date most of the research concerned with exploring the use of the skin for communication has focused on tactile displays. Such devices take many different forms from gloves or belts worn on the hand or around the waist and have been developed for a number of purposes, including spatial orientation and guidance, sensory substitution systems, notifications and alerts, and feedback on the success of control actions in human-computer interactions [Jones and Sarter 2008; Van Erp et al. 2005]. They are currently employed in application domains in which other communication channels, such as vision and audition, are either heavily taxed or in which visual displays are inconvenient or less appropriate to use. In addition to its tactile sensors, the skin houses thermal receptors that respond to changes in skin temperature and convey information to the central nervous system about the magnitude and rate of change in temperature. Thermal feedback may potentially be of use as a dedicated channel of communication or in enhancing tactile feedback in multisensory displays. Using the human thermal sensory system as a medium of communication presents unique challenges due to the spatial and temporal properties of this system which differ from those of other sensory systems. Although this constrains the types of cues that can be presented to users, it also opens up the possibility of creating new forms of feedback which by virtue of their novelty may be quite compelling in attracting users' attention.

To date, most of the thermal displays that have been developed have been used to present thermal cues that can assist in identifying an unseen object in a real or simulated environment. These displays attempt to reproduce the thermal sensations associated with making contact with the real object which vary as a function of the thermal properties of the object such as its thermal diffusivity [Bergmann Tiest and Kappers 2009]. The objective of the display is to assist in object recognition in situations in which visual information may be limited or absent, or to create a more realistic experience of the contact between the hand and an object in a virtual environment. Such displays typically consist of thermoelectric coolers, thermal sensors, and a temperature control system that monitors and controls the surface temperature of the thermal display [Jones and Ho 2008; Yamamoto et al. 2004]. Another application of thermal displays in which there is no physical contact between the device and the user is in virtual environments in which methods of heat transfer such as convection and radiation are used to create a greater sense of realism or "presence" in a simulated environment. Examples of this type of application include the use of infrared lamps to convey cues about the location of a virtual sun for visually impaired people being trained to navigate in

unfamiliar environments [Lecuyer et al. 2003], and employing lamps and ventilators to simulate the effects of walking past a fire blazing in a fireplace or an open window in a virtual environment [Dionisio et al. 1997]. In comparison to the critical evaluations that have been conducted on thermal displays and their use to facilitate object recognition [Ho and Jones, 2007, 2008; Kron and Schmidt, 2003], there are few quantitative studies that have demonstrated the importance of incorporating thermal stimuli in large-scale virtual environments.

Thermal interfaces can also be used to enhance user interactions with objects presented on digital media [Nakashige et al. 2009] or to present scalar information that is mapped onto temperature [Wettach et al. 2007]. For example, it seems feasible that variables such as pressure, distance or flow could be represented thermally, although the appropriate mapping between temperature and other scalar variables awaits further investigation. One early device called the Displaced Temperature Sensing System (DTSS) was designed to use temperature as a cue for encoding the position of the hand or fingers of a remote manipulator or prosthetic hand [Zerkus et al. 1994]. The authors proposed that signals from remote sensors on a manipulator could be sent to the device and drive thermodes on the fingers of the operator. Few studies have examined the feasibility of using thermal cues to encode abstract information and most of the devices that have been built to explore this possibility have not undergone rigorous human-use studies [MacLean and Roderick 1999; Wettach et al. 2007]. Two of the limitations associated with using thermal cues to represent abstract concepts is the relatively small number of sensations evoked by changes in skin temperature and the time taken by users to perceive changes in skin temperature within the innocuous range of temperatures (18-43 °C).

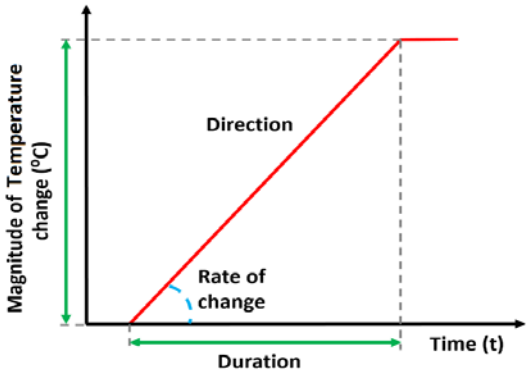

Fig. 1. Stimulus dimensions used to create thermal icons – direction (warming or cooling), intensity (magnitude of temperature change), rate and duration of temperature change.

Thermal displays have been used to create thermal icons by analogy to tactile icons or tactons in the tactile domain [Azadi and Jones 2014; Brown et al. 2005]. Thermal icons can potentially be created by varying the direction (warming or cooling), amplitude, spatial extent and duration of thermal stimulation as depicted in Figure 1. A few studies of thermal icons have been conducted using stimuli that varied with respect to the amplitude and rate of temperature change. These experiments showed that the direction of temperature change (i.e. warming or cooling) was the most salient feature of a thermal icon, that cooling was easier to detect than warming and that the rates at which the thermal stimuli were presented affected the time to detect stimuli [Halvey et al. 2012; Wilson et al. 2011]. No measurements were made of the change in skin temperature in response to these thermal inputs although the thermal display was set at 32 °C so as to maintain skin temperature relatively constant between trials. The overall performance of participants in identifying the four icons presented in these experiments varied from 64% to 83% correct [Wilson et al. 2012, 2013].

The properties of the human thermal sensory system provide the framework for designing thermal icons. The two primary types of thermal sensors in the skin, cold and warm thermoreceptors, vary with respect to the range of temperatures that they respond to, their innervation density across the body and the conduction velocities of their afferent fibers that transmit information within the CNS [Spray 1986]. Thermal sensitivity maps of the skin differ from homologous maps of tactile acuity in that the face is the most thermally sensitive region, and on the hand the thenar eminence at the base of the thumb is more sensitive to changes in both cold and warmth than the fingertips [Stevens and Choo 1998]. All areas of the body are more

sensitive to cold as compared to warmth, and due to differences in the conduction velocities of their afferent fibers (cold: 2-3 m/s, warmth: 1-2 m/s), cold stimuli are responded to more rapidly than warm stimuli [Yarnitsky and Ochoa 1991].

In an initial experiment on thermal icon identification, Singhal and Jones [2015] asked participants to identify six thermal stimuli presented on the thenar eminence on the hand using a visual template. The stimuli varied with respect to the direction, magnitude and rate of temperature change and each stimulus was presented for 30 s. The results indicated that these thermal icons were relatively easy to identify with an overall group mean of 91% correct and a mean Information Transfer (IT) of 2.26 bits.

A further series of experiments has been conducted to evaluate thermal pattern identification on the hand and arm and to determine which features of thermal stimuli can potentially be encoded by thermoreceptors in the skin and perceived by the user. On the basis of the findings from the first two sets of experiments described here which provided insight into the thermal dynamics of the skin's responses and subsequent perceptual processing, a third study was performed using system identification techniques to identify the impulse response function between the thermal input and response of the skin.

2 EXPERIMENT 1

The experiment was an absolute identification study in which participants had to identify which of six thermal patterns was presented on the tips of the index and middle fingers. These stimuli had been used in an earlier experiment where they were presented on the thenar eminence, one of the most thermally sensitive regions of the glabrous surface of the hand [Singhal and Jones 2015]. One of the objectives of the present experiment was to determine whether the ability to identify thermal patterns changes as a function of the thermal sensitivity of the area where the stimuli are presented.

2.1 Participants

Eight normal healthy individuals, 6 males and 2 females, ranging in age from 20 to 27 years old (mean: 25 years) participated in the experiments. They were all right-handed. They had no known abnormalities of the skin or peripheral sensory or vascular systems. None of the participants had any significant experience in thermal stimuli pattern recognition. They all signed an informed consent form that was approved by the MIT Committee on the Use of Humans as Experimental Subjects.

2.2 Apparatus

A thermal display was built using a thermoelectric module (Model TE-127-1.0-2.5, TE Technology, Inc.), 30-mm in length and width and with a thickness of 4.8 mm, mounted on a heat sink and fan. The Peltier module's temperature was controlled using a portable controller unit (Model TC-720, TE Technology, Inc.) run by a dual-mode power supply. Two thermistors, 457 μm in diameter and 3.18 mm in length (Model 56A1002-C8, Alpha Technics), were used, one of which was mounted on the surface of the thermal display for feedback control of the device's temperature and the other measured the temperature of skin on the fingertip in contact with the display as illustrated in Figure 2. The input to the feedback controller was the temperature of the display rather than skin temperature so that the same stimulus was delivered to all participants and the temperature of the skin was essentially the same at the start of each trial.

A LabVIEW-based (National Instruments) graphical user interface (GUI) was used to send commands to the controller for the thermal display and to record skin temperature continuously at 20 Hz. A second computer was used to run a GUI in LabVIEW on which the participants' responses were recorded.

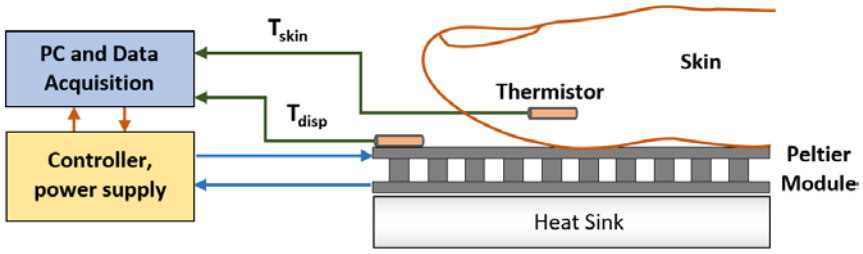

Fig. 2. Schematic illustration of the thermal display with the Peltier module mounted on a heat sink, and the thermistors measuring the temperatures of the module and the skin on the fingertip.

2.3 Thermal Stimuli

Thermal stimuli were designed by varying the amplitude and rate of change in temperature. Three basic thermal profiles (square wave, step and ramp) were used, each of which had two values to give a total of six patterns. The duration of each stimulus was 30 s. A schematic illustration of the patterns that participants used to indicate their responses is shown in Figure 3. The waveforms depicted were not intended to be precise in terms of the actual stimuli delivered but served to emphasize the differences among the patterns. The time and temperature axes did not have numeric values on them when viewed by participants. The dotted red line represents the baseline skin temperature of 32 °C. Patterns A and F were based on a square wave input, B and D were linearly decreasing and increasing ramps, respectively, and C and E were based on a step input. The average rate of change of temperature was 3 °C/s for A and F, 0.7 °C/s for B and D, and 2 °C/s for C and E. The direction and intensity of the changes in temperature differed in the above pairs to make them more distinguishable. The temperature ranged between 24 and 38 °C for A and C, and 18 and 32 °C for E and F. The direction of the 18 °C change in temperature for B and D was reversed.

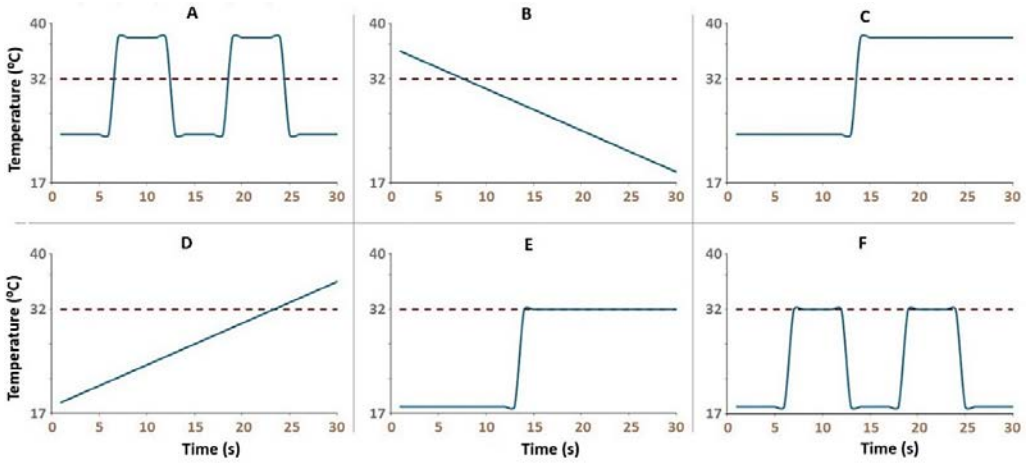

Fig. 3. Visual depiction of the six thermal patterns that varied with respect to the intensity and rate of change in temperature. The dashed line indicates the baseline skin temperature. In the template that participants viewed there were no numeric values on the axes.

2.4 Procedure

Prior to starting the experiment participants washed their hands. A thermistor was then glued to the edge of the index finger using biocompatible cyanoacrylate (Liquid Bandage™, Johnson & Johnson). Initial skin temperatures ranged from 29 to 33

°C with a mean of 30 °C. The ambient temperature in the room was maintained at 24 °C, as measured with a thermocouple in free air. Participants placed the tips of their right index and middle fingers on the surface of the thermoelectric module. The contact area of the fingers on the thermal display ranged from 600-750 mm^2 across participants. A visual depiction of the stimuli was presented on the computer screen in front of the participant (see Figure 3). In the familiarization period participants selected each stimulus in turn using a computer mouse and the stimulus was then presented on the fingers while they viewed the visual display. After this, there was a series of practice trials in which stimuli were presented and participants had to indicate which pattern they felt. Feedback was provided after each response. After the practice session which typically lasted 5 minutes, the experiment began. To ensure that the skin temperature of the hand returned to a baseline temperature before each stimulus was presented, the thermal display was maintained at 30 °C for 20 s between trials.

Each stimulus lasted 30 s and was presented eight times in a randomized order to give a total of 48 trials. Two different auditory cues were provided to signal the start and finish of each stimulus presentation. After the second auditory cue, participants indicated their responses by selecting the letter (A-F) associated with the visual pattern on the GUI on the screen. Responses had to be made within 10 s and on most trials participants made their responses within a couple of seconds. A rest break was provided when requested. No feedback regarding the correctness of the responses was provided during the main experiment.

2.5 Results

The group mean temperatures measured on the index finger and the thermal display during the experiment are shown in Figure 4. As is evident in the figure, the display temperature remained constant at 30 °C between trials and the skin temperature was generally within 1 °C of the display temperature. Although the skin temperature tracked that of the display it changed more slowly and so did not reach the minimum and maximum temperatures presented. Across the six patterns presented the group mean percentage of correct responses ranged from 75% to 85% correct with an overall mean of 80% correct. These data are shown in Figure 5 together with those from the earlier experiment using the same stimuli but presented on the thenar eminence. For the latter site, the group mean was 91% correct responses (range: 80-98%). At both sites Pattern B, which involved a linear decrease in temperature was the easiest stimulus to identify with 100% correct responses, whereas pattern D which was a linear increase in temperature from cold to warm had the lowest percent of correct responses at 64%. Due to the inhomogeneity of the variance a non-parametric ANOVA (Friedman's test) was conducted on these percent correct scores. The results indicated that there was a significant main effect of thermal stimuli ($p=0.005$). Post hoc analyses revealed that pattern B had a significantly higher number of correct responses than pattern D.

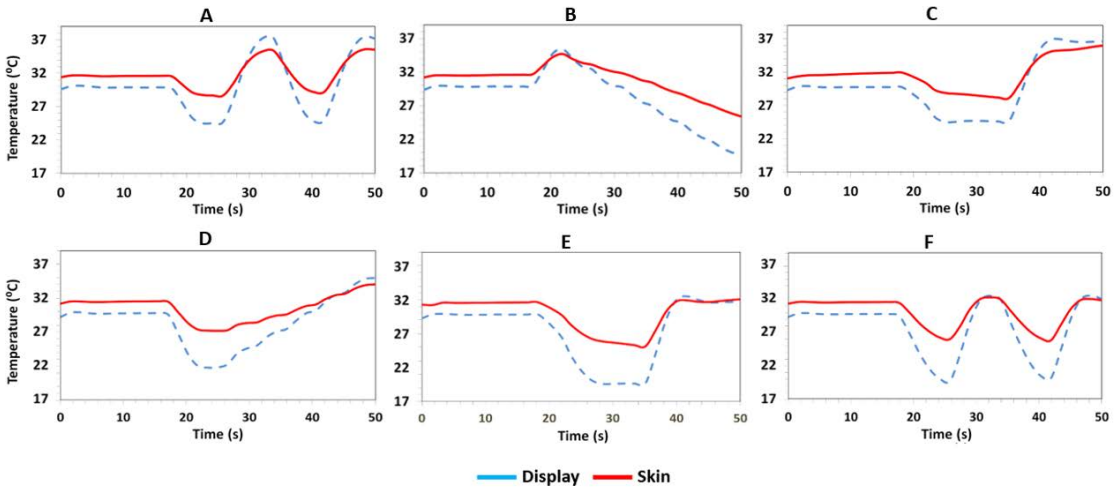

Fig. 4. Group mean temperature measured on the skin and the display averaged across trials for each of the six thermal stimuli. The first 20 s of data prior to each stimulus presentation are also shown.

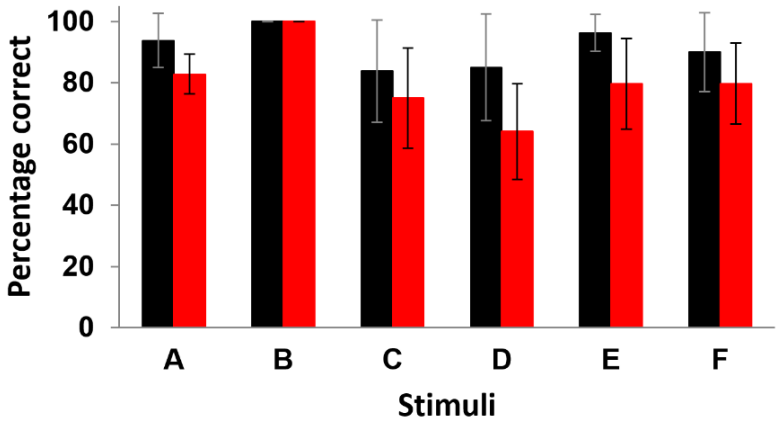

Fig. 5. Group mean percent correct responses for each thermal pattern when presented on the thenar eminence (black) and the fingertips (red). The standard deviations are shown.

The confusion matrix of the participants' responses shown in Table 1 indicates that participants confused patterns A and F which were both square waves with different magnitudes. Pattern C was often misidentified as pattern D; these two patterns varied with respect to the rate at which temperature changed. The information transfer (IT) was calculated from the confusion matrix of each participant using the equations in Tan et al. [2010]. IT values specify how many bits of information participants can distinguish from the set of patterns presented and indicate the maximum number of stimuli that can be identified without error. The maximum IT for six stimuli is 2.6 bits and 2^{IT} gives the maximum number of stimuli that can be correctly identified. The IT values calculated from the confusion matrix from each participant ranged from 1.66 to 2.02 bits across participants with a group mean of 1.83 bits. This is interpreted as indicating that for this set of six stimuli 3.6 patterns can be correctly identified.

Table 1. Confusion matrix of the group responses with scores out of the total of 64 trials presented for each stimulus. The highlighted diagonal represents correct responses.

Stimuli ▼	**Responses ►**					
	A	**B**	**C**	**D**	**E**	**F**
A	53	0	2	0	0	11
B	0	64	0	0	0	0
C	0	0	48	13	3	0
D	0	0	6	41	17	0
E	0	0	4	9	51	0
F	13	0	0	2	1	51

2.6 Discussion

These results indicate that thermal icons created by varying the direction, magnitude and rate of temperature change can be reliably identified with little training with performance comparable to that reported for tactile icons delivered at a single location on the hand [Azadi and Jones 2014; Brown et al. 2005]. A comparison of the present results on the fingertips with those from an earlier experiment using the same thermal stimuli presented on the thenar eminence and with the same contact area, indicates that participants found it easier to identify the stimuli when presented on the thenar eminence [Singhal and Jones, 2015]. This is reflected in both the higher percentage of correct responses on the thenar eminence (91% vs 80%) and higher IT values (2.26 bits vs 1.83 bits). As noted in the Introduction, the sensitivity of the thenar eminence to changes in temperature is superior to that of the fingertips and differences as small as 0.03-0.09 °C in the amplitudes of two cooling pulses

can be resolved on the thenar eminence [Johnson et al. 1973]. However, the perception of suprathreshold stimuli is not necessarily related to the capacity to detect stimuli at threshold levels. For vibrotactile stimuli it has been shown that tactons are in fact more accurately identified on the forearm as compared to the finger [Azadi and Jones 2014; Summers et al. 2005], despite the higher density of mechanoreceptors in the fingertips and their associated superior tactile acuity.

The overall performance of participants in the present experiment is comparable to that reported in other studies that have used smaller sets of thermal icons and much shorter presentation times [e.g. Wilson et al. 2012]. The decision to use a longer duration was based on pilot study data that showed that for inputs such as square waves a long presentation time was required for the stimuli to be represented in the thermal response of the skin. These preliminary studies also indicated that sinusoidal, square-wave and triangular-wave inputs would probably not be able to be distinguished perceptually as the changes in skin temperature for each of these signals was fairly similar. As the data shown in Figure 4 indicate the pattern of results for the thenar eminence and the fingers was essentially the same in terms of which stimuli were easier and more difficult to identify which provides insight into how subsequent thermal icons should be designed. The accuracy with which pattern B was identified (100 %) suggests that a linear decrease in temperature is very easy to identify. Although pattern D involved a linear increase in temperature there was an initial decrease in skin temperature towards the starting temperature as shown in Fig. 4 which makes that pattern more complex than the former.

IT values are dimensionless and independent of task conditions and so are a useful metric to compare information processing across experiments and sensory modalities [Jones and Tan 2013]. The mean IT of 1.83 bits in this experiment was lower than that measured for the same patterns presented on the thenar eminence (IT 2.26 bits) which implies that the higher sensitivity of the thenar eminence to threshold-level changes in temperature assists the perception of supra-threshold stimuli. These IT values are within the range reported for other haptic variables such as vibration (2.4 bits), force (1.5 bits) and stiffness (1.7 bits) [Azadi and Jones 2014, Cholewiak et al. 2008]. The channel capacity of the thermal sensory system is therefore comparable to that of the other cutaneous senses which have been explored much more intensively as communication systems [Jones 2011, Wall and Weinberg 2003]. The dimensionality of tactile stimuli has been shown to affect information transfer with estimates suggesting 1-2 bits per dimension [Rabinowitz et al. 1987]. The thermal stimuli in the present experiment varied along three dimensions: direction, amplitude and rate although these were not varied orthogonally. This makes it difficult to discern whether participants were able to respond to the rate of temperature range independently of its amplitude. In general, it has been found across sensory modalities that multidimensional channel capacities are typically less than the sum of the unidimensional capacities [Durlach et al. 1989].

Several aspects of the present experiment limit the findings in terms of their potential for application in thermal displays. First, the length of the stimuli at 30 s imposes an unrealistic burden on a user focused on responding to the stimuli in a timely manner. The time taken to process thermal information is longer than that for other aspects of cutaneous stimulation [Lederman and Klatsky 1997], which means a high throughput is not realistic for thermal icons. Nevertheless, shorter highly salient thermal icons can be designed on the basis of these results and possibly implemented as part of a multimodal cutaneous communication system. Second, the poorer performance on the fingertips as compared to the thenar eminence means that thermal displays should be mounted on areas of the body with high thermal sensitivity such as the thenar eminence or the wrist. Finally, in the context of developing thermal icons that users can readily identify better performance may be achieved by presenting the same relative thermal stimuli to users (i.e. ± 5 °C from the baseline skin temperature), given the human variability in resting skin temperatures on the extremities [Verrillo et al. 1998].

3 EXPERIMENT 2

Improvements to the design of thermal icons are required if they are to be used effectively in a thermal display for communication. In the second experiment the duration of the icons was shortened and the temperature profile delivered was determined by the user's skin temperature. In the first experiment the same absolute change in temperature was presented to all participants. The skin temperature was recorded at the periphery of the contact area to monitor the change in skin temperature during contact with the display but was not used as an input to the thermal display. In order to present the same change in temperature to all users, the thermal stimuli should be presented relative to the user's skin temperature. Such a set of thermal icons should induce similar thermal sensations by presenting the same temperatures to all users. In the context of our longer-term objective of developing a wearable thermal display it was decided to build a display that could be worn around

the wrist which is one of the most thermally sensitive regions in the upper extremity. In the present experiment a revised set of thermal icons was designed that were shorter in duration (8 s) and presented relative to each participant's baseline skin temperature.

3.1 Participants

Ten normal healthy individuals ranging in age from 20 to 28 years old (mean: 25 years) participated in the experiments. They were all right-handed. They had no known abnormalities of the skin or peripheral sensory or vascular systems. None of the participants had any significant experience in thermal stimuli pattern recognition. They all signed an informed consent form that was approved by the MIT Committee on the Use of Humans as Experimental Subjects.

3.2 Apparatus

A wrist-strap based thermal display was developed using a thermoelectric module (Model TE-83-1.0-1.5, TE Technology, Inc.) mounted on a water-cooled copper heat sink. The thermoelectric module was a 22 mm long and 19 mm wide Peltier device, with a thickness of 3.8 mm, giving a contact area of 418 mm^2. The water-cooled heat sink was a CNC milled copper water block (Model WBA-1.00-0.49-CU-01, Custom Thermoelectric) with a cross-section of 25 mm x 25 mm and a thickness of 12 mm. The water block was connected to a 200 ml water tank (80 mm x 60 mm x 60 mm) made from laser cut acrylic sheets; a continuous flow of water in the assembly was maintained by a DC brushless submersible water pump (Model DC30A-1230, ZKSJ) with dimensions of 40 mm x 40 mm x 30 mm. The water-based cooling system was chosen in preference to a fan based system as it provided more rapid cooling and did not result in any vibration sensations on the wrist.

Three thermistors, 457 µm in diameter and 3.18 mm in length (Alpha Technics) similar to those used in Experiment 1were used in the experiment. One thermistor was mounted on the surface of the thermal display for feedback control of the device's temperature. Two other thermistors measured the temperature at two locations on the skin. A photo and schematic of the thermal display with thermistors and the control setup is shown in Figure 6. The thermistor at location 1 measured the temperature of the Peltier module's surface. There was an insulation layer on one side to prevent thermal contact with the skin and thus reduce the error in measuring the display temperature. The thermistor at location 2 measured the skin temperature at the edge of the contact area of the skin with the Peltier module. This measurement indicated the change in skin temperature due to the thermal stimulus presented on the thermal display. A baseline temperature measurement on the wrist was given by the thermistor at location 3. This measurement differed for each participant and was unaffected by the thermal stimuli due to its location. The wrist mounted fixture for holding the Peltier module and the heat sink was fabricated using a rapid prototyping system. The fixture was designed such that it could fit comfortably on the wrist and then fastened so that it did not move. The surfaces of the Peltier module and thermistors were made flush with the surface of the fixture in contact with the skin.

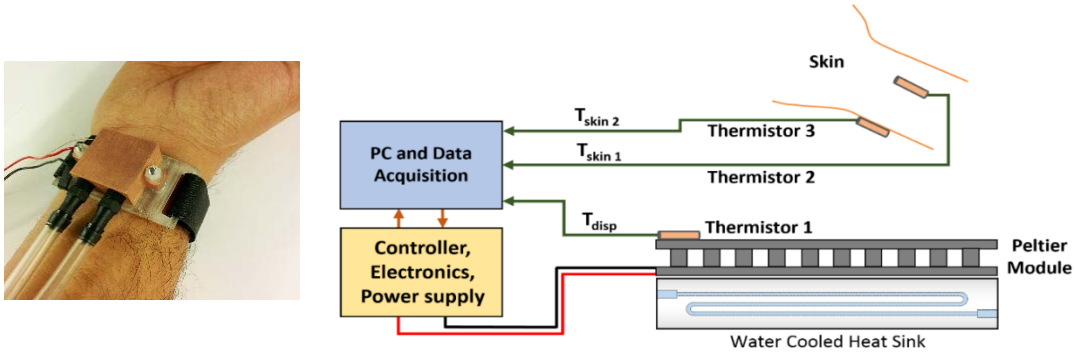

Fig. 6. Photo of the display on the wrist and schematic illustration of the thermal display with the Peltier module mounted on a water-cooled heat sink, and thermistors measuring the temperatures of the module and of the skin on the wrist.

Data acquisition and feedback control of the Peltier device was done using National Instruments data acquisition modules (Model NI cDAQ-9174, NI 9263, NI 9474, NI9205). A LabVIEW-based (National Instruments) graphical user interface (GUI) was used to send commands to control the Peltier module, and to record the skin temperature continuously at 1 kHz. The baseline skin temperature was the input to the controller at the start of each trial and was used as the reference temperature when the thermal stimulus was presented so that the same relative stimulus was delivered to all participants. A second computer was used to run a GUI on which the participants' responses were recorded.

3.3 Thermal Stimuli

Similar to the stimuli used in the first experiment, this set of thermal patterns was designed by varying two stimulus dimensions, the amplitude and rate of change in temperature. The initial temperature (T_i) was set at the baseline skin temperature, which means that the magnitude of the change in temperature was relative to the temperature measured at thermistor 3. Each of the three basic thermal profiles (square wave, step and ramp) provided a different rate of temperature change and varied in direction (warming or cooling) to give a total of six patterns as shown in Figure 7. The intensity (ΔT) was fixed at 6 °C for both warming and cooling. The duration of each of the six patterns was 8 s preceded by a 5 s calibration period in which the thermal display was maintained at the baseline skin temperature as measured by thermistor 3. Patterns A and D were based on a square wave input, B and E a step input, and C and F were linearly decreasing and increasing ramps. The average rate of change of temperature was 3 °C/s for A and D, 1.5 °C/s for B and E, and 0.7 °C/s for C and F. The maximum rate of change of the temperature was limited by the dynamics of the thermal display system. The difference in the direction of temperature change (warming or cooling) in the above pairs made them distinguishable.

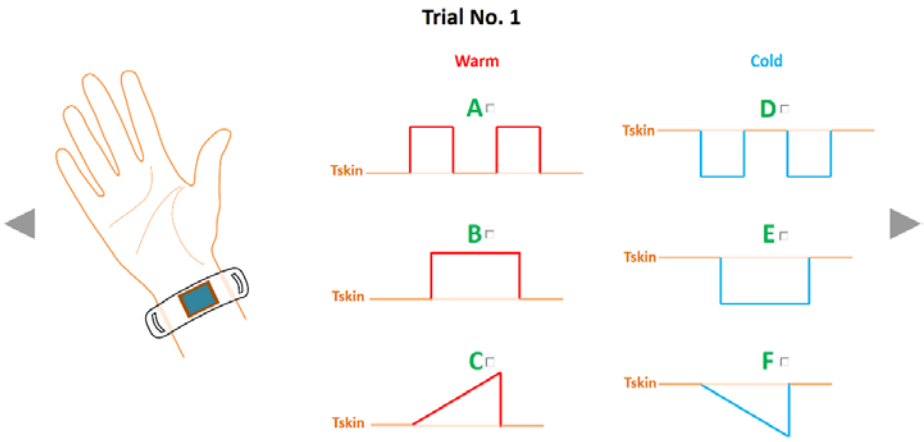

Fig. 7. Screen shot of the GUI presented on the computer screen in front of the participants with each of the six thermal patterns. Participants indicated their responses by selecting the pattern using a computer mouse.

3.4 Procedure

Prior to starting the experiment, the procedure was explained to participants and the thermal display was placed on the wrist and then the strap was comfortably tightened. Participants read the instructions on the computer screen. They were then familiarized with the thermal patterns that would be presented. In the familiarization period participants selected each stimulus in turn using a computer mouse and the stimulus was presented on the wrist while they looked at the visual display. After this, there was a series of practice trials in which stimuli were presented and participants had to indicate which pattern they felt. Feedback was provided after each response. After the practice session which typically lasted 5 minutes, the experiment began. The participants' initial skin temperatures ranged from 30 to 32 °C with a mean of 31 °C. The ambient temperature was maintained at 25 °C, as measured with a thermocouple in free air. The thermal display was maintained at the baseline skin temperature between trials before each stimulus was presented.

Each stimulus was presented eight times in a randomized order to give a total of 48 trials. Two different auditory cues were provided to signal the start and finish of each stimulus presentation. After the second auditory cue, participants indicated their responses by selecting the checkbox beside the letter (A-F) associated with the visual pattern on the GUI on the screen (see Figure 7). Responses had to be made within 10 s and on most trials participants made their responses within a couple of seconds. After every six trials, participants switched the display to the other wrist in order to avoid any adaptation effects. A rest break was provided when requested. No feedback regarding the correctness of the responses was provided during the main experiment.

3.5 Results

The temperatures measured on the three thermistors averaged across all the participants are shown in Figure 8. The plots include temperature measurements during the first 5 s of the trial which is the initial calibration period. These data clearly indicate that thermistor 2 records the change in skin temperature during stimulus presentation and that there is a delay in the skin's response and in the gain. The temperature measured by thermistor 3 on the skin but not in contact with the display is the baseline skin temperature which did not change during stimulus presentation indicating the localized response of the skin to thermal stimulation.

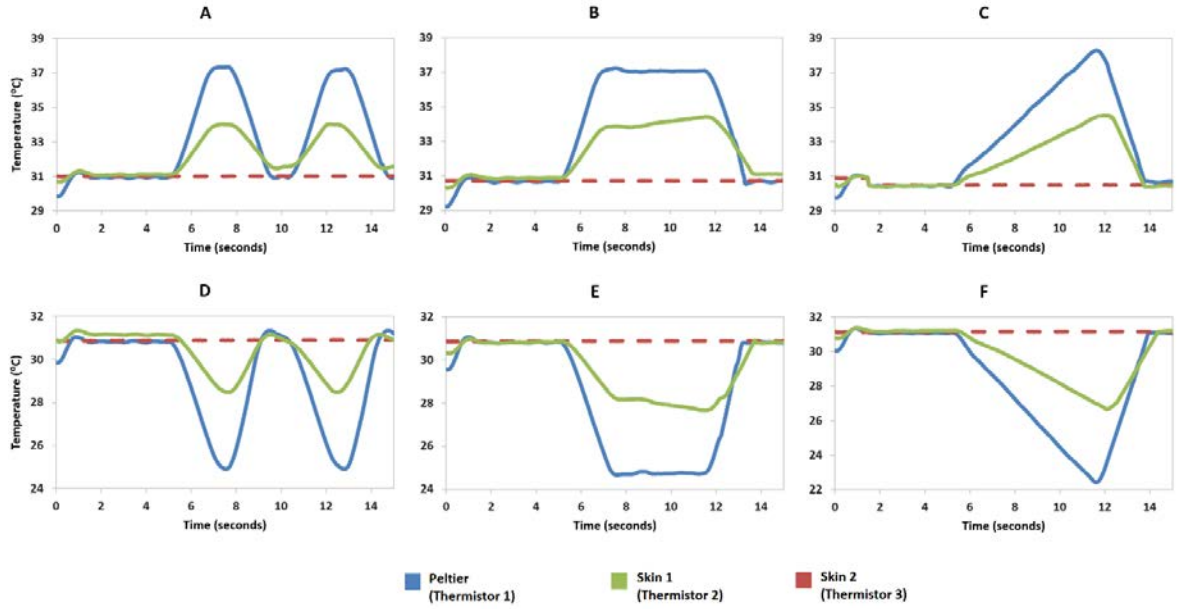

Fig. 8. Temperatures measured on the Peltier module and at two locations on the wrist averaged across trials and subjects for each of the six thermal stimuli. The first 5 s indicate the calibration period.

The percentage of correct responses for each stimulus averaged across stimuli and participants ranged from 73% to 100% correct with an overall mean of 89% correct. Figure 9 shows the mean percentage of correct responses for each of the six stimuli. Patterns A and D which were based on a square wave profile and had two temperature pulses were the easiest stimuli to identify with 99% and 100% correct responses across participants. Pattern F, which was a linear decrease and then increase in temperature from cold to warm had the lowest percentage of correct responses at 73%. Pattern B which was a step change from the baseline skin temperature to a warm temperature was also one of the more difficult patterns to identify with 81% correct.

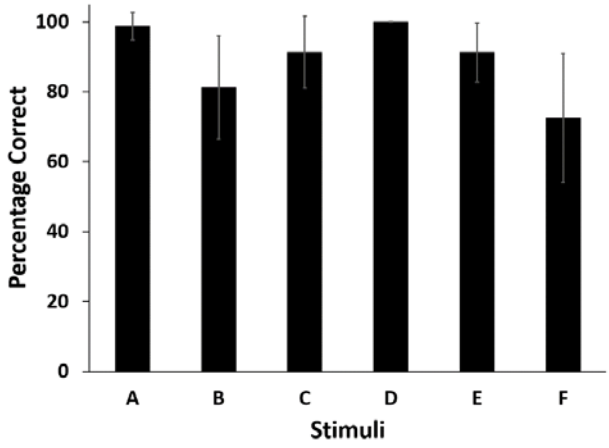

Fig. 9. Group mean percent of correct responses for each thermal pattern. The standard deviations are shown.

When the thermal patterns are grouped in terms of those that warmed (A, B and C) or cooled (D, E and F) the skin, the overall performance of participants is similar with 90% correct for patterns that warmed and 88% correct for those that cooled the skin. In terms of the input waveforms, that is the square wave, step and ramp functions, performance was best for the square wave function at 99% correct, followed by 86% correct for the step function and 82% correct for the ramp input. These three inputs can also be differentiated on the basis of the rate of change in temperature which was highest for the square wave at 3 °C/s, followed by the step (1.5 °C/s) and ramp (0.7 °C/s) functions. A non-parametric ANOVA (Friedman's test) was conducted on these data and indicated that there was a significant main effect of thermal stimuli on identification ($p<0.001$). Post-hoc tests (Wilcoxon signed ranks) indicated that the score for pattern F was significantly lower than those for patterns A, C, D and E and pattern B was identified less accurately than patterns A, C and D.

Table 2. Confusion matrix of the group responses with scores out of the total of 80 trials presented for each stimulus. The highlighted diagonal represents correct responses.

	Responses					
Stimuli	**A**	**B**	**C**	**D**	**E**	**F**
A	79	1	0	0	0	0
B	4	65	10	0	1	0
C	0	7	73	0	0	0
D	0	0	0	80	0	0
E	0	0	0	1	73	6
F	0	0	0	0	22	58

The confusion matrix of the participants' responses is shown in Table 2. Patterns that were the hardest to identify, B and F, were misidentified as C and E respectively suggesting that participants found it difficult to determine the differences in the rates with which skin temperature was changing (see Fig. 8). The IT values calculated from the confusion matrix from each participant ranged from 1.98 to 2.6 bits with a group mean value of 2.13 bits. This is interpreted as indicating that for this set of 6 stimuli 4.4 patterns can be correctly identified.

3.6 Discussion

The results from the present experiment indicate that the performance of participants is similar to that observed in the earlier experiment on the thenar eminence using a different set of icons where the mean score was 91% correct [Singhal and Jones 2015]. Performance is better than the 83% correct reported by Wilson et al. [2012] who presented four icons on the thenar

eminence that varied with respect to intensity and direction. The stimulus durations in these two studies are comparable (8 s and 10 s) which suggests that when thermal icons are designed based on the responses of the skin they can be accurately identified with little training. The revised set of thermal icons was created using three distinct input temperature profiles: a square wave, step and ramp. The range of temperatures and rates of change in temperature were modified from those used in the earlier experiments to create a more distinguishable set of six patterns which were shorter in duration. Continuous measurement of skin temperature during stimulus presentation indicated that features of the input, for example the step versus ramp, were captured in the skin's response (see Fig. 8) and presumably the associated sensations.

The overall performance in the present experiment supports the use of thermal displays in applications in which the device can be worn around the wrist. The present configuration uses an external water tank and pump for cooling in addition to the water-cooled heat sink on the wrist device. Obviously for a wearable system the cooling capabilities for the thermoelectric module will need to be included in the display itself. Future designs of this display will incorporate either a micro-fluidic system or other forms of active cooling system.

The rate at which skin temperature changes does affect thermal thresholds but provided it is faster than 0.1 °C/s it has little effect on the ability to detect changes in temperature [Kenshalo 1976, Kenshalo et al. 1968; Yarnitsky and Ochoa, 1991]. Faster rates of change have also been shown to decrease the time to detect a stimulus [Wilson et al. 2011]. In the present experiment three rates of change were used to create the thermal patterns (0.7, 1.5 and 3 °C/s) and these were assumed to be perceptually distinct. As noted in the Results (Section 3.5), the input waveform varied with the rate at which the temperature changed and so it is not possible to attribute the superior identification performance for the highest rate (3 °C/s) solely to this factor. It seems more likely that the double pulse in the square wave input made it more salient than the other two input waveforms.

The effectiveness of the revised set of six thermal icons used in this experiment was evaluated in terms of IT values. The mean IT of 2.13 bits is higher than the 1.83 bits reported in the first experiment and is comparable to that measured for tactons delivered at a single location on the body [Azadi and Jones 2014]. For vibrotactile stimuli better identification performance has been achieved when the spatial location of the stimuli is used as a stimulus dimension [Jones et al. 2009]. Spatial summation is pervasive in the thermal senses and participants are often unable to discriminate between two thermal inputs displayed on a single fingertip [Yang et al. 2009] or to perceive varying stimulus amplitudes across the fingers [Green 1977]. This suggests that distributing thermal stimuli across the skin may be much less effective for the thermal as compared to the tactile modality. However, recent studies on spatio-temporal illusions involving the thermal sensory system indicate that it is possible to change the perceived location of thermal stimulation by varying the temporal interval between stimuli [Singhal and Jones 2016]. Such interactions could possibly be used to increase the dimensionality of thermal icons in thermal displays.

The results from these two experiments on thermal icons indicate that with appropriate design of the stimulus parameters it is possible to create a set of thermal patterns that can be reliably identified. Characterization of the relation between the thermal input from the display and the response of the skin is important for further development of these patterns in that the process of design then becomes model-based instead of empirical. The final experiment was designed to quantify the relation between thermal inputs and changes in skin temperature using system identification techniques.

4 SKIN THERMAL SYSTEM IDENTIFICATION

It is evident from the skin temperature data in the previous experiments (e.g., Figures 4 and 8) that there is a delay in the response of the skin to the thermal stimulus, and that the skin temperature changes at a slower rate than the display temperature due to lower bandwidth of the skin. A system characterization experiment that captured the dynamics of the skin's thermal response would provide insights regarding the skin as a thermal system. An understanding of these thermal characteristics would allow for the development of dynamic models that could predict the change in skin temperature for any given thermal input. In the present experiment characterization of the skin's thermal system was performed using linear system identification techniques [Ljung 1999]. A temperature profile with a defined frequency range, duration, and amplitude was designed that could capture the dynamic properties of the skin's thermal response. Thermal sensors on the Peltier module and the skin provided the input-output data used in these analyses.

4.1 Experimental Setup

The wearable thermal display developed for the previous experiment was used to characterize the skin's thermal system. A schematic of the cross-section of the thermal display mounted on the wrist with the locations of the thermistors is shown in Figure 10. The experimental setup was the same as that used in Experiment 2, except that only two thermal sensors were used, one on the skin and the other on the Peltier module. A LabVIEW based user interface generated the input voltage signal (peak amplitude 3 V) to drive the Peltier module and sampled the signals from the two thermistors. The sampling frequency was 1 kHz. The excitation signal and the data from both thermistors were written to a measurement file. MATLAB (Mathworks, Inc.) was used to conduct the system identification analysis. This experiment was conducted with five participants. All the parameters of thermal stimulation were constant across participants.

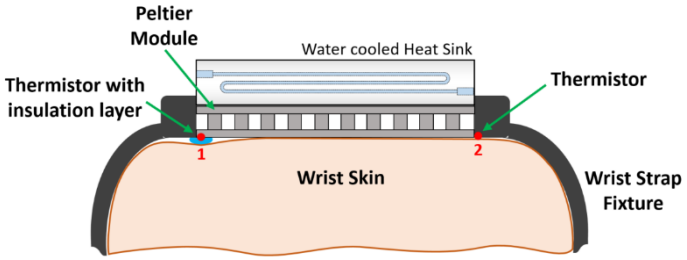

Fig. 10. Schematic of the cross-section of the thermal display mounted on the wrist skin

4.2 System Identification Analysis

The system was perturbed by a broadband stochastic signal while the resulting temperatures of the Peltier module and skin were measured. From these data the non-parametric impulse response function was estimated using linear system identification techniques. A binary stochastic signal was used to drive the Peltier temperature controller via an H-bridge current amplifier and the two voltage signals (V_D and V_S) from the thermistors were recorded. The temperature of the Peltier module (T_D) serves as the input to the skin and the temperature of the skin (T_S) is the output of the system. The output voltage signals (V_D and V_S) from the thermal sensors on the Peltier module and skin were used as the inputs and outputs in the skin system identification analysis. A block diagram of the system with the stochastic (g(t)), binary (u(t)), input (x(t)) and output (y(t)) signals is shown in Figure 11.

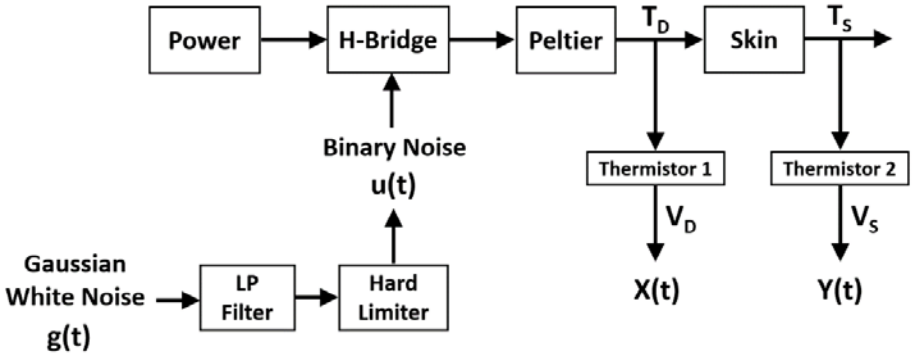

Fig. 11. Block diagram of the testing apparatus with the stochastic binary signal to the h-bridge and output voltages recorded from the thermistor at the Peltier (V_D) and at the skin (V_S).

The input signal to the electronics was generated by filtering a stochastic Gaussian white noise signal, g(t), by a first-order, low pass filter and then hard-limiting it (see Eq. 1) to produce a broadband stochastic binary signal, u(t).

$$u(t) = u_b = \begin{cases} 0, & x_{gwn} < 0 \\ 1, & x_{gwn} \geq 0 \end{cases} \quad (1)$$

The duration of the Gaussian white noise signal was 300 s. This length was based on pilot studies that indicated that it was sufficient to capture the dynamics of the skin's thermal system. The frequency band of the broadband stochastic signal was 0.2 to 0.6 Hz. The upper limit of the frequency band was determined by the dynamics of the Peltier module and the lower limit was chosen to keep the change in the temperature of the Peltier module within the innocuous range of skin temperatures.

The input binary signal and measured sensor voltage signals were re-centered around zero by subtracting the dataset means and removing any linear trend lines, if present. The input binary signal was used by the H-bridge to control the Peltier module's heating and cooling. The H-bridge was configured to work as a switch to control the direction of the temperature change of the Peltier device. Its temperature increased for values of the binary signal greater than zero, and decreased for values below or equal to zero. The power electronics was set up in conjunction with the H-bridge to keep the Peltier device powered on throughout the signal. Figure 12 shows the centered and de-trended voltage signals from the thermistors on the Peltier module and the skin.

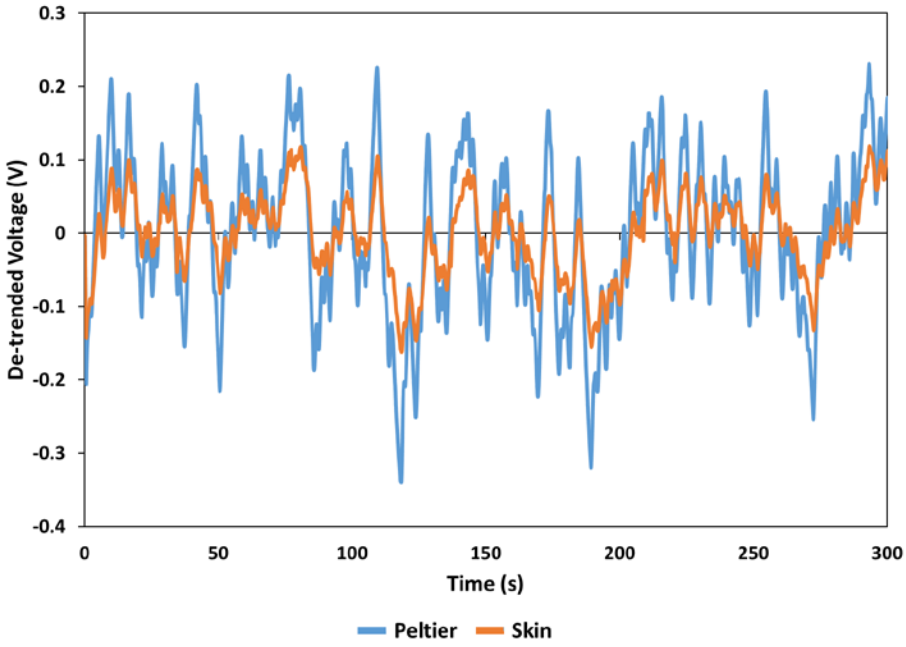

Fig. 12. Output signals recorded from thermistors on the Peltier module and the skin. The signals were centered and de-trended.

The centered and de-trended datasets were analyzed to calculate the natural response of the skin system. In system identification analysis the non-parametric response of the system is estimated and then fitted with a parametric impulse response function to arrive at a mathematical model of the system. First, the autocorrelation of the input signal to the skin was calculated using Equation (2), where x_i is the voltage signal (V_D) representing the input temperature to the skin system.

$$C_{xx} = \frac{1}{N+1}\sum_{i=j}^{N}\left(x_{i-j} \cdot x_i\right) \quad (2)$$

The cross-correlation of the temperature signal (V_D) input to the skin system and the skin output signal (V_S) dataset was calculated using Equation (3), y_i is the output voltage signal from the thermistor at the skin.

$$C_{xy} = \frac{1}{N+1}\sum_{i=j}^{N}(x_{i-j} \cdot y_i) \tag{3}$$

From the input autocorrelation vector, the Toeplitz matrix was constructed using Equation (4).

$$T_{j,k} = C_{xx_{|j-k|}} \tag{4}$$

The natural or impulse response function of the system was calculated using Equation (5) where inverse of the Toeplitz is multiplied with the cross-correlation vector and the sampling interval (Δt).

$$h_{est} = \frac{1}{\Delta t}.{T_{j,k}}^{-1} \cdot C_{xy} \tag{5}$$

were h_{est} is the estimated impulse response function of the skin system. This non-parametric impulse response vector was fit to the parametric impulse response model of a linear system. The fit was achieved by minimizing an objective function F shown in equation (6) as the sum of square errors between the estimated impulse response (h_{est}) and the parametric model of the response (h_{model}).

$$F = \sum_{i=1}^{N}(h_{est} - h_{model}(i\Delta t))^2 \tag{6}$$

4.3 Results

A comparison of the non-parametric or estimated impulse response function of the system with a parametric linear system model was performed using MATLAB. The objective function shown in Equation (6) was minimized using the non-linear least squares Levenberg-Marquardt minimization algorithm. This was implemented in MATLAB to obtain estimates of the various parameters of the linear system transfer function. A transfer function with 3 poles and a single zero was optimal and provided the best fit to the data. Figure 13 shows the plot of the estimated impulse response function and the parametric model for the skin system.

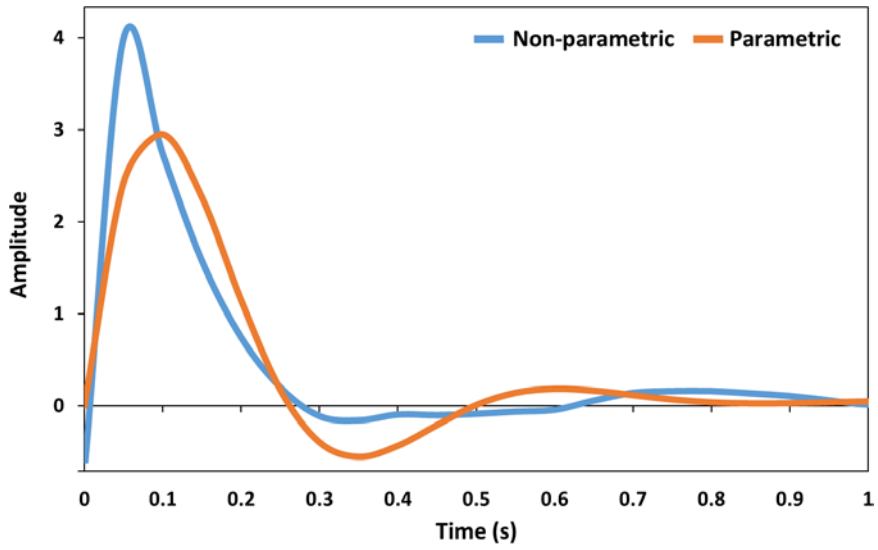

Fig. 13. Comparison of the non-parametric (estimated) and parametric impulse response functions for the skin.

To compare the fit of the parametric impulse response function with the estimated function, the VAF (Variance Accounted For) of the non-parametric (VAF_{est}) and the parametric (VAF_{model}) impulse response functions were calculated using Equation (7).

$$VAF_{est} = 100.\left(1 - \frac{var(y_{est,i} - y_i)}{var(y)}\right) \tag{7}$$

$$VAF_{model} = 100.\left(1 - \frac{var(y_{model,i} - y_i)}{var(y)}\right)$$

$$where: y_{est,i} = \Delta t.\sum_{i=j}^{N}(h_{est,i} \cdot x_{i-j}) \ and \ y_{model,i} = \Delta t.\sum_{i=j}^{N}(h_{model,i} \cdot x_{i-j})$$

The VAF_{model} and VAF_{est} were calculated to be 98.41% and 98.72% respectively. The values of VAF for both the functions are close to 100% indicating that the non-parametric and parametric impulse response functions captured the dynamics of the skin thermal system well.

The measured temperature signals from the skin were compared with the predicted thermal response from the parametric and non-parametric impulse response functions. The error between the measured and predicted signals was also calculated. Figure 14 shows the plot of the measured and predicted output signals, together with the error between them. System identification analysis was conducted on all the data sets from the five participants tested. The models were compared across participants and were found to be very similar with the VAF for the estimated and modeled functions varying between 95.4% and 99.6%.

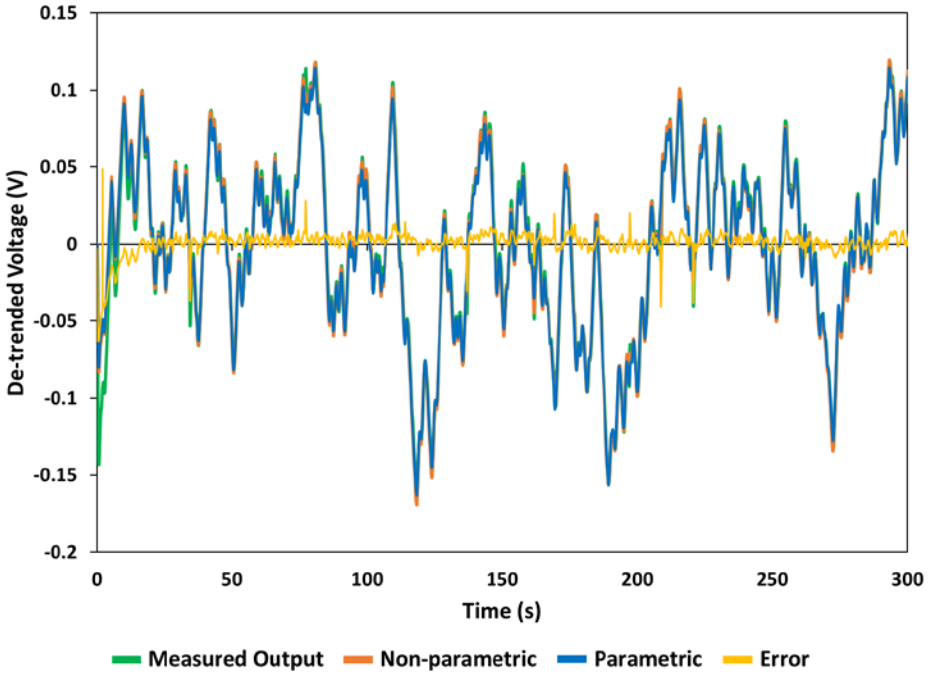

Fig. 14. Comparison of the output skin temperature signals between measured signal (green), output predicted by non-parametric impulse response function (orange), parametric impulse response function (blue) and the error between measured and the predicted output (yellow).

The thermal characteristics of the skin as reflected in the parametric impulse response function can be used to predict the changes in skin temperature for any thermal input. The data from Experiment 2 were used to determine the accuracy of the parametric model in estimating the change in skin temperature to a given thermal input, since the thermal display and skin site tested were the same as in the present study. The skin temperature output was calculated by convolving the temperature input signal from the Peltier module, which was given in the form of one of the six thermal patterns, with the parametric model determined from system identification. The predicted change in skin temperature from the model was compared to the measured skin temperature for each of the six thermal patterns. These results are shown in Figure 15 for one representative pattern (pattern A). The model predicts the change in skin temperature in an unrelated experiment with a very different thermal input well, indicating that this analytic approach captures the dynamics of the skin's thermal response.

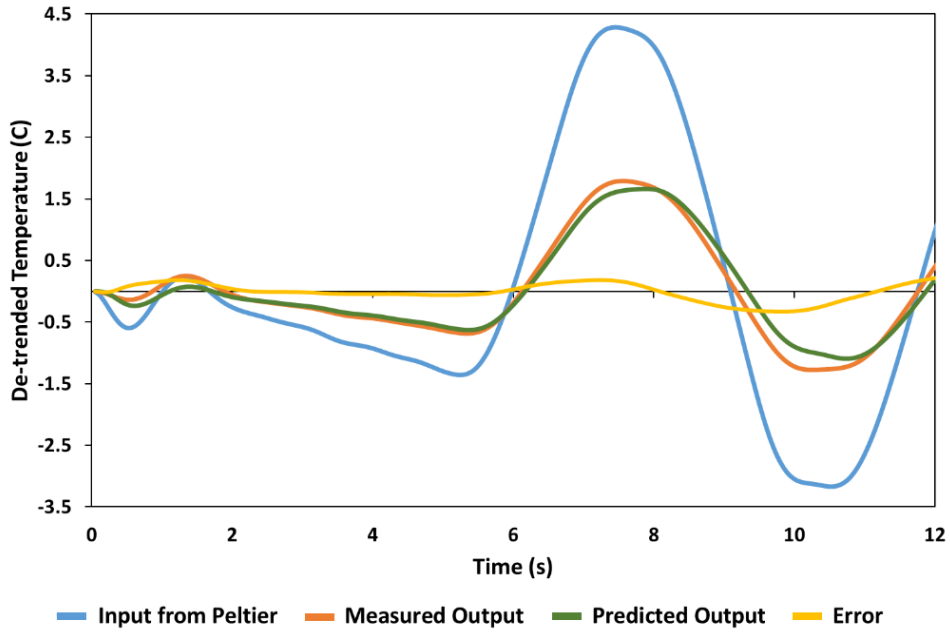

Fig. 15. Comparison of the measured (orange) and predicted (green) output skin temperature for Pattern A in Experiment 2. The predicted skin temperature signal was determined by convolving the input temperature signal from the Peltier device (blue) with the parametric model determined from the system identification experiment.

4.4 Discussion

The results from the system identification study indicate that the thermal response of the skin can be represented by as a linear dynamic system. A third-order linear system model fitted to the non-parametric impulse response function gives a VAF value of 98.4% indicating an accurate fit. The excellent fit of the predicted signals with the measured output signals from the skin indicate the fidelity of the mathematical model, which was verified using data sets from five participants. The utility of the model is demonstrated by the accuracy with which it could predict the change in skin temperature in Experiment 2 in which the input to the skin was one of six thermal icons. This suggests that the response of the skin thermal system can be predicted for any given input temperature. The successful characterization of the relation between the thermal input from the display and the response of the skin can now be used to develop more effective thermal icons by focusing on model-based design rather than the empirical approach followed to date.

The skin thermal response model developed in this experiment includes the effects of both warm and cool temperature stimulations as the input signal from the Peltier device covered the full range of changes in temperature and thus can be employed irrespective of the nature of the thermal input. The skin thermal model depends on the site on the body where the

stimuli were applied and so it is anticipated that there will be variations in the parameters of the linear dynamic model at different locations. The model developed in this study corresponds to the linear system for the skin on the wrist, and no difference was noted between the left and right wrists.

The predicted skin temperature change can be used in conjunction with a model that characterizes the physical and perceptual correspondence for dynamic thermal stimulation. Using 0.5 Hz and 1 Hz periodic warming and cooling simulation profiles, Ho et al. [2016] found that the delay between the physical and perceived onset of the changes in temperature was 318 ms for cold and 460 ms for warm, consistent with the known faster neural response to cooling of the skin [Yarnitsky and Ochoa 1991]. In contrast the perceived peaks of the warm and cold periodic stimuli differed for warming and cooling. For cool stimulation, the subjective peak preceded the physical temperature peak, whereas for warm stimuli the subjective peak always followed the corresponding physical peak. A preliminary model of the temporal filtering properties of the thermal senses was developed by Ho et al. [2016]. Such a model would be enhanced by using a broader bandwidth of stimulation profiles and a tailored thermal input derived from linear dynamic models.

5 CONCLUSIONS

A series of experiments has been conducted to determine the feasibility of creating thermal patterns that could potentially become part of a cutaneous communication system. The results from the first set of experiments indicated the importance of measuring the actual changes in skin temperature while the thermal patterns are presented as some features of the inputs may not be represented in the thermal response of the skin and so are unlikely to be useful building blocks for icons. These experiments also revealed that sites other than the fingertips can be used effectively to identify thermal icons and that the greater thermal acuity of the thermal eminence and the forearm as compared to the fingertips [Stevens and Choo 1998] is also reflected in their superior capacity to process suprathreshold stimuli. Even when the duration of the icons was substantially shortened from 30 s to 8 s, participants were still able to identify the patterns when presented on the wrist with high levels of accuracy (89% correct).

The thermal icons in both experiments were created by varying the direction (warming or cooling), magnitude and rate of temperature change presented on the display. There was no difference in performance when identifying warm or cool stimuli and although icons with faster rates of temperature change were easier to identify than those with slower rates this variable was confounded with the type of input waveform (square wave, step and ramp), so both variables may have contributed to facilitating identification. It is generally reported that all body regions are more sensitive to cold than warmth, with warm thresholds often being twice as large as cold thresholds [Harding and Loescher 2005, Stevens and Choo 1998]. Such threshold effects did not influence the perception of supra-threshold cold and warm stimuli in the present experiments. The high level of performance of participants in these experiments was surprising given reports of the poor spatial and temporal acuity of the thermal senses [Green 1977, Ho et al. 2017]. It must be noted that participants' attention was focused on the stimuli being presented and that they identified the patterns using a visual representation of the stimuli, both of which would have aided performance. Nevertheless, these findings suggest the feasibility of using thermal cues either in isolation or in conjunction with other tactile signals in communication systems.

The system identification experiment was conducted so that a dynamic model of the skin's thermal response could be developed that could predict the change in skin temperature for a given thermal input. Such a model would greatly facilitate the development of thermal icons which are at present empirically determined and validated [Wilson et al. 2012, 2013]. The non-parametric and parametric impulse response functions provided excellent fits to the experimental data and more importantly were able to predict the changes in skin temperature from an unrelated experiment at the same location with thermal icons. The dynamic model provides a means of determining a priori the effect of changing various thermal parameters on skin temperature.

In conclusion, these experiments offer insight into information processing in the thermal senses and how this sense may be used in the context of cutaneous communication systems. Further work will need to determine how the perceptibility of thermal icons changes when other sensory information must also be attended to and if the concurrent presentation of tactile cues facilitates or impedes the perception of changes in skin temperature.

REFERENCES

[1] M. Azadi and L.A. Jones. 2014. Evaluating vibrotactile dimensions for the design of tactons. *IEEE Transactions on Haptics* 7, 14-23.

[2] W.M. Bergmann Tiest and A.M.L. Kappers. 2009. Tactile perception of thermal diffusivity. *Attention, Perception & Psychophysics* 71, 481-489.

[3] L.M. Brown, S.A. Brewster, and H.C. Purchase. 2005. A first investigation into the effectiveness of tactons. *Proceedings of the first joint Eurohaptics Conference and the Symposium on Haptic Interfaces for Virtual Environments and Teleoperated Systems* 167-176.

[4] S.A. Cholewiak, H.Z. Tan, and D.S. Ebert. 2008. Haptic identification of stiffness and force magnitude. *Proceedings of the Symposium on Haptic Interfaces for Virtual Environment and Teleoperator Systems*, 87-91.

[5] J. Dionisio, V. Henrich, U. Jakob, A. Rettig, and R. Ziegler. 1997. The virtual touch: Haptic interfaces in virtual environments. *Computers & Graphics* 21, 459-468.

[6] N.I. Durlach, H.Z. Tan, N.A. Macmillan, W.M. Rabinowitz, and L.D. Braida. 1989. Resolution in one dimension with random variations in background dimensions. *Perception & Psychophysics* 46, 293-296.

[7] B. G. Green. 1977. Localization of thermal sensation: An illusion and synthetic heat. *Perception & Psychophysics* 22, 331-337.

[8] M. Halvey, M. Henderson, S.A. Brewster, G. Wilson, and S.A. Hughes. 2012. Augmenting media with thermal stimulation. *Proceedings of the Haptic and Audio Interaction Design Conference* LNCS 7468, 91-100.

[9] L.M. Harding and A.R. Loescher. 2005. Adaptation to warming but not cooling at slow rates of stimulus change in thermal threshold measurements. *Somatosensory and Motor Research 22*, 45-48.

[10] H.-N. Ho and L. A. Jones. 2007. Development and evaluation of a thermal display for material identification and discrimination. *ACM Transactions on Applied Perception* 4, 1-24.

[11] H.-N. Ho and L. A. Jones. 2008. Modeling the thermal responses of the skin surface during hand-object interactions. *Journal of Biomechanical Engineering* 130, 21005-1-8.

[12] H.-N. Ho, K. Sato, S. Kuroki, J. Watanabe, T. Maeno, and S.Y. Nishida. 2017. Physical-perceptual correspondence for dynamic thermal stimulation. *IEEE Transactions on Haptics 10,* 84-93.

[13] K. O. Johnson, I. Darian-Smith, and C. LaMotte. 1973. Peripheral neural determinants of temperature discrimination in man: A correlative study of responses to cooling skin. *Journal of Neurophysiology* 36, 347-370.

[14] L.A. Jones. 2011. Tactile communication systems: Optimizing the display of information. *Progress in Brain Research* 192, 113-128.

[15] L.A. Jones and H.-N. Ho. 2008. Warm or cool, large or small? The challenge of thermal displays. *IEEE Transactions on Haptics* 1, 53-70.

[16] L.A. Jones, J. Kunkel, and E. Piateski. 2009. Vibrotactile pattern recognition on the arm and back. *Perception* 38, 52-68.

[17] L.A. Jones and N.B. Sarter. 2008. Tactile displays: Guidance for their design and application. *Human Factors* 50, 90-111.

[18] L.A. Jones and H.Z. Tan. 2013. Application of psychophysical techniques to haptic research. *IEEE Transactions on Haptics* 6, 268-284.

[19] D. R. Kenshalo. 1976. Correlations of temperature sensitivity in man and monkey, a first approximation. In *Sensory Functions of the Skin with Special Reference to Man*, Y. Zotterman (Ed.). Pergamon Press, Oxford, 305-330.

[20] D.R. Kenshalo, C. E. Homes, and P.B. Wood. 1968. Warm and cool thresholds as a function of rate of stimulus temperature change. *Perception & Psychophysics* 3, 81-84.

[21] D A. Kron and G. Schmidt. 2003. Multi-fingered tactile feedback from virtual and remote environments. *Proceedings of the 11th International Symposium on Haptic Interfaces for Virtual Environments and Teleoperated Systems* 16-23.

[22] A. Lecuyer, P. Mobuchon, C. Megard, J. Perret, C. Andriot, and J. Colinot. 2003. Homere: A multimodel system for visually impaired people to explore virtual environments. *Proceedings of IEEE Virtual Reality* 251-258.

[23] S. J. Lederman and R. L. Klatzky. 1997. Relative availability of surface and object properties during early haptic processing. *Journal of Experimental Psychology: Human Perception and Performance* 23, 1680-1707.

[24] L. Ljung. 1999. *System Identification: Theory for the User*. Prentice Hall, Upper Saddle River, NJ.

[25] K.E. MacLean and J.B. Roderick. 1999. Smart tangible displays in the everyday world: A haptic doorknob. *Proceedings of the IEEE/ASME International Conference in Advanced Intelligent Mechatronics* 203-208.

[26] M. Nakashige, M. Kobayashi, Y. Suzuki, H. Tamaki, and S. Higashino. 2009. “Hiya-Atsu” media: Augmenting digital media with temperature,” *Proceedings of the Computer-Human Interaction Conference* 3181-3186.

[27] W.M. Rabinowitz, A.J.M. Houtsma, N.I. Durlach, and L.A. Delhorne. 1987. Multidimensional tactile displays: Identification of vibratory intensity, frequency, and contactor area. *Journal of the Acoustical Society of America* 82, 1243-1252.

[28] A. Singhal and L.A. Jones. 2015. Dimensionality of thermal icons. *IEEE World Haptics Conference* 469-474.

[29] A. Singhal and L.A. Jones. 2016. Space-time interactions and the perceived location of cold stimuli. *IEEE Haptics Symposium* 92-97.

[30] D.C. Spray. 1986. Cutaneous temperature receptors. *Annual Reviews in Physiology* 48, 625-638.

[31] J.C. Stevens and K.C. Choo. 1998. Temperature sensitivity of the body surface over the life span. *Somatosensory and Motor Research* 15, 13-28.

[32] I.R. Summers, J.J. Whybrow, D.A. Gratton, P. Milnes, B.H. Brown, and J.C. Stevens. 2005. Tactile information transfer: A comparison of two stimulation types. *Journal of the Acoustical Society of America*, 118, 2527-2534.

[33] H.Z. Tan, C.M. Reed, and N.I. Durlach. 2010. Optimum information-transfer rates for communication through haptic and other sensory modalities. *IEEE Transactions on Haptics* 3, 98-108.

[34] J.B.F. Van Erp. 2005. Presenting directions with a vibrotactile torso display. *Ergonomics* 48, 302-313.

[35] R. T. Verrillo, S. J. Bolanowski, C. M. Checkosky, and F. P. McGlone. 1998. Effects of hydration on tactile sensation. *Somatosensory and Motor Research* 15, 93-108.

[36] C. Wall, III and M.S. Weinberg. 2003. Balance prostheses for postural control. *IEEE Engineering in Medicine and Biology Magazine* March/April, 84-90.

[37] R. Wettach, A. Danielsson, C. Behrens, and T. Ness. 2007. A thermal information display for mobile applications. *Proceedings of the Mobile Human-Computer Interaction Conference '07*, 182-185.

[38] G. Wilson, M. Halvey, S.A. Brewster, and S.A Hughes. 2011. Some like it hot? Thermal feedback for mobile devices. *Proceedings of the Computer-Human Interaction Conference* 2555-2564.

[39] G. Wilson, S. Brewster, M. Halvey, and S. Hughes. 2012. Thermal icons: Evaluating structured thermal feedback for mobile interaction. *Proceedings of the Mobile Human Computing Interaction Conference* 309-312.

[40] G. Wilson, S. Brewster, M. Halvey, and S. Hughes. 2013. Thermal feedback identification in a mobile environment," *Proceedings of the Haptic and Audio Interaction Design Conference* LNCS 7989, 10-19.

[41] A. Yamamoto, B. Cros, H. Hasgimoto, and T. Higuchi. 2004. Control of thermal tactile display based on prediction of contact temperature. *Proceedings of the International Conference on Robotics and Automation*, 1536-1541.

[42] G. Yang, L.A. Jones, and D. Kwon. 2008. Use of simulated thermal cues for material discrimination and identification with a multi-fingered display. *Presence* 17, 29-42.

[43] D. Yarnitsky and J.L. Ochoa. 1991. Warm and cold specific somatosensory systems. *Brain* 114, 1819-1826.

[44] M. Zerkus, B. Becker, J. Ward, and L. Halvorsen. 1994. Thermal feedback in virtual reality and telerobotic systems. *Proceedings of the Fourth International Symposium on Measurement and Control in Robotics* 107-113.

Received May 2017; revised Month YYYY; accepted Month YYYY.